MNRAS **000**, 1–15 (2019) Preprint 30 March 2022 Compiled using MNRAS LATEX style file v3.0

Revisiting bright δ Scuti stars and their period–luminosity relation with *TESS* and *Gaia* EDR3

Natascha Barac[1]★, Timothy R. Bedding[1,2]†, Simon J. Murphy[1,2] and Daniel R. Hey[1,2]
[1]*Sydney Institute for Astronomy, School of Physics, University of Sydney 2006, Australia*
[2]*Stellar Astrophysics Centre, Department of Physics and Astronomy, Aarhus University, 8000 Aarhus C, Denmark*

Accepted 16 April 2019.

ABSTRACT
We have used NASA's TESS mission to study catalogued δ Scuti stars. We examined TESS light curves for 488 stars, including many for which few previous observations exist. We found that 54 are not δ Scuti pulsators, with most instead showing variability from binarity. For the 434 δ Scuti stars, we list the period and amplitude of the dominant pulsation mode. Using Gaia EDR3 parallaxes, we place the stars in the period–luminosity diagram. We confirm previous findings that most stars lie on a ridge that corresponds to pulsation in the fundamental radial mode ridge, and that many fall on a second ridge that is a factor two shorter in period. This second ridge is seen more clearly than before, thanks for the revised periods and distances. We demonstrate the value of the period–luminosity diagram in distinguishing δ Scuti stars from short-period RR Lyrae stars, and we find several new examples of high-frequency δ Scuti stars with regular sequences of overtone modes, including XX Pyx and 29 Cyg. Finally, we revisit the sample of δ Scuti stars observed by Kepler and show that they follow a tight period–density relation.

Key words: parallaxes – stars: variables: delta Scuti – stars: oscillations

1 INTRODUCTION

High-precision photometry from the *Kepler* and *TESS* space missions is revolutionizing the study of pulsating stars (for recent reviews, see Aerts 2021; Kurtz 2022). Combining this photometry with distances measured with Gaia brings new opportunities to investigate period–luminosity (P–L) relations. The P–L relations of classical pulsators have a long history, particularly with Cepheids (Leavitt & Pickering 1912) and RR Lyr variables, making these stars indispensable distance indicators. More recently, P–L relations for their main-sequence cousins—the δ Scuti stars—have been revisited using parallaxes from Gaia to refine the luminosities (Ziaali et al. 2019; Jayasinghe et al. 2020; Poro et al. 2021). However, in many cases the catalogued periods were determined decades ago from ground-based photometry. The *TESS* spacecraft is collecting high-precision all-sky photometry, enabling us to measure pulsation periods more precisely and homogeneously than ever before, without atmospheric variability or large daily gaps in the time series.

We have used *TESS* light curves to study catalogued δ Sct stars, including many for which few ground-based observations exist, in order to confirm their status and measure their dominant pulsation modes. We use our revised data, together with Gaia EDR3 parallaxes, to place these targets more accurately in the period–luminosity diagram. We build on the work of Ziaali et al. (2019), who used targets from the heterogeneous Rodríguez et al. (2000) catalogue, plus targets observed in the *Kepler* mission, to examine the P–L relation for δ Sct stars.

The construction of our sample is described in Sec. 2. Our procedures for analysing *TESS* data and measuring the dominant pulsation mode of each star are outlined in Sec. 3. In Sec. 4 we plot the P–L relation of our sample and outline its value in distinguishing δ Sct stars from other pulsators, and from non-pulsating stars. We also show the period–density relation for *Kepler* δ Sct stars (Sec. 4.2) and discuss the excess of stars having a dominant pulsation period that is half that of the predicted fundamental mode (Sec. 4.1), as identified by Ziaali et al. (2019). In Sec. 5, we discuss stars belonging to the class of high-frequency δ Sct stars investigated by Bedding et al. (2020).

2 SAMPLE CONSTRUCTION

Our sample of stars is drawn primarily from the catalogue of Rodríguez et al. (2000, hereafter R2000). In a comprehensive review and compilation of known δ Sct stars (up to January 2000), R2000 catalogued the primary observational properties of 636 stars, including their dominant pulsation periods and visual magnitudes. We only considered the 407 stars with $V < 12$ mag. The *TESS* spacecraft observed 371 stars from this list in its first three years (Sectors 1–39). Of these, 264 were observed at 2-min cadence in at least one sector, and the remaining 107 stars only have full-frame

★ E-mail: nbarac@sas.upenn.edu
† E-mail: tim.bedding@sydney.edu.au

image (FFI) data available, which has 30-minute cadence for Sectors 1–26 and 10-minute cadence from Sector 27 onwards. These 371 stars are all included in our sample.

We supplemented our sample with targets from the compilation of 1578 δ Sct stars by Chang et al. (2013, hereafter C2013), which contains 860 δ Sct stars not present in R2000. Of these, we analysed the 117 stars with $V < 12$ mag that have 2-minute *TESS* data available in Sectors 1–39. Our final sample therefore contains 371 stars from R2000 and 117 additional stars from C2003.

3 PULSATION PERIODS

3.1 *TESS* light curves

We queried the *TESS* data products available on the Mikulski Archive for Space Telescopes (MAST)[1] for each star using the Python Lightkurve package (Lightkurve Collaboration et al. 2018). We downloaded all available light curve data products for 2-min targets, whereas for targets with only FFI data we used the Lightkurve wrapper Platypus[2] to extract and correct the time-series data. In both cases, we used all available data from *TESS* Sectors 1–39.

We computed the Fourier transform of each light curve in order to measure the dominant pulsation modes. Due to the non-zero *TESS* integration times, the measured amplitudes are smaller than the intrinsic amplitudes. To account for this averaging, sometimes referred to as 'smearing' or 'apodization', we divided the measured Fourier amplitudes by the function $\mathrm{sinc}\,(\pi\nu t_{\mathrm{int}})$, where t_{int} is the integration time. Because there is no dead time between integrations, this equation can be written as $\mathrm{sinc}\left(\frac{\pi}{2}\frac{\nu}{t\nu_{\mathrm{Nyq}}}\right)$ (e.g., Huber et al. 2010; Murphy 2012). We note that this correction is more important for the light curves made with 30-min FFI data.

A simple peak-finding algorithm was used to extract the peak with the largest corrected amplitude (i.e. the dominant mode) for each star. This was adequate for our goals, given our focus is identifying δ Sct stars and measuring the dominant modes, rather than carrying out a full frequency analysis on every star. We limited the search to peaks above 3 d^{-1} to capture pressure mode (p-mode) pulsations. Below this limit, pulsation peaks are typically gravity or Rossby modes. The Fourier spectra of stars with dominant peaks below 5 d^{-1} were also inspected to confirm that the peak was due to δ Sct (p-mode) pulsations.

The period–luminosity relation outlined in Section 3 was also used as a guide to confirm that we were recording the correct pulsation modes. Stars that fell significantly to the right of the P–L relation (that is, those with periods too long to be δ Sct pulsations) were inspected to confirm their variability. A number of these stars were identified as binaries showing no evidence of δ Sct pulsations. Other stars were able to be amended with the correct δ Sct pulsation mode. For example, the highest peak in the spectrum of BR Hyi was in fact due to binarity; upon inspection there are clear δ Sct pulsations and so the dominant δ Sct mode was manually recorded.

These results are compiled in Table 1, which lists the dominant pulsation mode that we have measured in each star from the *TESS* data, along with the corrected amplitude.

[1] https://archive.stsci.edu/
[2] https://github.com/danhey/platypus

3.2 Non-pulsating Stars

Based on inspecting the *TESS* light curves and examining publications since R2000, we identified 54 stars from our sample that showed no evidence of δ Sct pulsations. Of these, 15 stars were included in the original R2000 catalogue and 39 were added from C2013. We give details on these stars below.

Ziaali et al. (2019) already flagged the following eight stars from R2000 as not having δ Sct pulsations, which we confirmed with *TESS* data:

- V753 Cen, TV Lyn, and UY Cam are RR Lyrae variables (e.g., McNamara 2011; Sneden et al. 2018);
- BQ Phe, DE Oct, and V345 Gem are binaries with no pulsating component (Liakos & Niarchos 2017);
- AK Men was also found to be a binary with no pulsating component; and
- V1228 Cen is a B-type β Cep variable (Pigulski & Pojmański 2008).

We identified an additional seven stars from the R2000 catalogue that are not δ Sct variables: V579 Per (appears to be an RR Lyr variable), TU UMi, HD 213272 (HR 8569, HIP 111041), FZ Vel (HD 77140, HR 3588), HD 10088 (HIP 7685), 18 Vul (HD 191747, HR 7711), V1241 Tau (HD 21102, WX Eri), and GS UMa (HD 90747).

Finally, we identified 39 non-δ Sct stars from the Chang et al. (2013) catalogue. A significant number of these stars are in binary systems with no pulsating component. Their Fourier spectra often look similar to those of high-amplitude δ Sct (HADS) stars and were initially flagged for inspection after placement in the P–L diagram, for falling outside of the expected area. Thus, we confirm the value of the P–L relation in helping to identify non-δ Sct pulsators that we might otherwise misclassify.

3.3 Comparison with published periods

Figure 1 compares the dominant pulsation mode recorded in the original catalogues with our values from *TESS*. The values agree well for the majority of our sample: periods for 71 percent of the stars are within 10% of the original value. It appears that stars with larger differences are primarily those with amplitudes smaller than 1 mmag. This is presumably a result of lower signal-to-noise ratio (SNR) and poorer time coverage of the ground-based observations, making it difficult to accurately identify and measure the dominant mode. Some δ Sct stars are also known to undergo amplitude modulation (see Bowman et al. 2016, and references therein), which may have caused a new mode to become dominant since the previous studies.

4 PERIOD–LUMINOSITY RELATION

Revising the dominant modes of our sample allows them to be placed more accurately in the period–luminosity diagram. We calculated the absolute magnitudes (M_V) for these stars using:

$$M_V = V + 5\log_{10}\pi + 5 - A_V\,, \tag{1}$$

where π is the parallax in arcsec. We used parallaxes from *Gaia* EDR3, except in the cases where the parallax from *Hipparcos* was more precise. The extinction due to interstellar dust (A_V) was calculated by fitting the spectral energy distribution (SED) of each

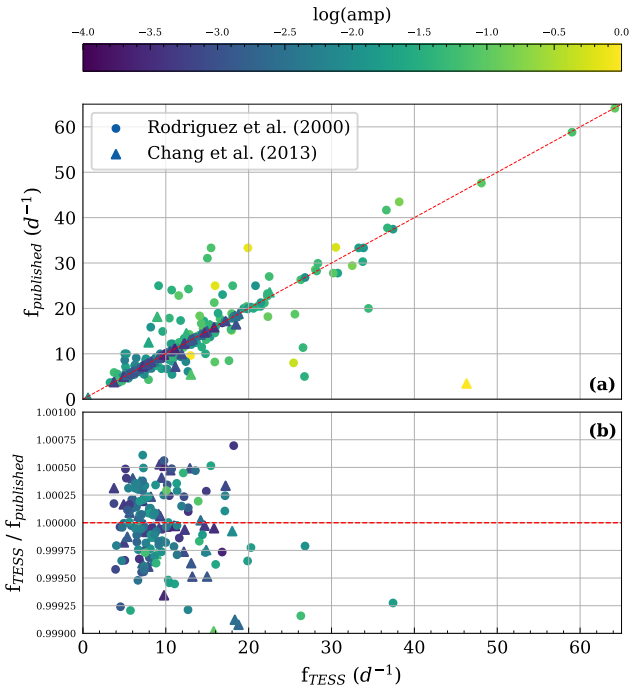

Figure 1. (a) Comparison between the catalogued frequencies and those measured from *TESS*. The red dotted line shows a ratio of 1:1. Stars included in the R2000 catalogue are plotted as circles, while those added from the C2013 catalogue are plotted as triangles. **(b)** Close-up of the ratios of values, highlighting stars whose *TESS*-revised dominant modes are close to their previously published values.

star using the astroARIADNE[3] python package. For each star, we queried photometric data from the Vizier database (Ochsenbein et al. 2000). The stars were then fitted to the Castelli & Kurucz (2003) model using a nested sampling algorithm (dynesty, Speagle 2020) to obtain extinctions. In order to obtain a uniform sample of apparent (V) magnitudes, we used Tycho V_T and B_T magnitudes converted to the Johnson V photometric system using the linear transformation

$$V = V_T - 0.090(B_T - V_T), \quad (2)$$

for which systematic errors do not exceed 0.015 mag (ESA 1997). In plotting, we further limited our sample to stars with fractional parallax uncertainties < 5%, and extinction A_V < 0.2 mag.

Figure 2 shows our updated period–luminosity relation, coloured by pulsation amplitude. The red labelled stars are RR Lyrae variables, which have their own P–L relation (McNamara 2011; Sneden et al. 2018; Molnár et al. 2022; Garofalo et al. 2022). Indeed, when accurate parallaxes are available, the P–L relation is a useful way to distinguish between short-period RR Lyr variables (so-called RRc stars, which pulsate in the first overtone) and HADS, whose light curves look very similar. The dashed diagonal line is the revised P–L relation derived by Ziaali et al. (2019):

$$M_V = (-2.94 \pm 0.06) \log P - (1.34 \pm 0.06). \quad (3)$$

This fit was based on periods from R2000 and parallaxes from Gaia DR2 and is very similar to the P–L relation derived by McNamara (2011), which was fitted to HADS stars thought to pulsate in their fundamental radial mode.

We see in Fig. 2 that higher-amplitude stars tend to fall closer to the fundamental-mode ridge, while lower-amplitude stars show more scatter. This main ridge is also sharper than that of Ziaali et al. (2019), and there are fewer stars falling to the lower right of the relation. Using our revised periods and distances has also made a second ridge, lying to the left of the fundamental-mode ridge, more distinct than before.

Figure 3 shows the horizontal distance of data points to Eq. 3 as a histogram. There is still a strong excess of stars displaced to the left by 0.3 in $\log P$, corresponding to a period ratio of 0.50. Since histogram results can depend on bin size, we also added a fixed-bandwidth kernel density estimate (KDE) for the same data to Fig. 3. The excess of stars displaced to the left of 0.3 in $\log P$ is still present in the KDE, indicating that the excess seen in the histogram is real.

4.1 Second Ridge Stars

Our revised P–L diagram highlights that a significant number of stars appear to have a dominant pulsation period that is half that of the fundamental mode. This excess of second-ridge stars was identified by Ziaali et al. (2019) but has not yet been explained. Figure 4 demonstrates that many can be classified as 'true' second ridge stars, where the dominant pulsation mode falls on the second ridge and we also identify a peak at the predicted fundamental mode. Conversely, some stars appear to only coincidentally lie on the second ridge. These are typical δ Sct and even HADS that are displaced, perhaps due to binarity or some other error in their absolute magnitudes.

We note, for example, the following stars that appear to be shifted vertically in absolute magnitude due to binarity:

- RS Cha (9 Cha; HD 75747) is a contact EB consisting of two pre-main-sequence stars with tidally perturbed pulsations (Steindl et al. 2021). Since these stars have similar luminosities, our absolute magnitude is too bright by about 0.7 mag and has shifted the star to the second ridge.
- BO Lyn looks like a typical HADS with main peak at 10.71 (60 ppt), plus weaker peaks at 16.47 (5 ppt) and 16.04 (4 ppt). We suspected it to be a binary, and therefore vertically displaced in absolute magnitude, as the dominant mode of HADS should fall on the fundamental-mode P–L sequence. Indeed, Li et al. (2018) suggested it has an A-type companion in a 35-yr orbit, based on variations in the pulsation phase over the past century.
- ρ Tau (HD 28910) is a member of the Hyades, with a Hipparcos parallax of 20.61 mas which matches the cluster. It lies above the cluster isochrone in the colour-magnitude diagram, and Antonello & Pasinetti Fracassini (1998) say that is a binary and there is probably a photometric effect due to the companion. Hence, it is probably shifted up and not a true second-ridge star.

These exceptions are few: the majority of stars on the second ridge are not binaries. Furthermore, we confirm the finding by Ziaali et al. (2019) that known binary systems do not lie preferentially on the second ridge.

An alternative explanation may come from amplitude modulation and mode resonances. We have discussed amplitude modulation on the timescales of decades as contributing to changes between the measurements from our source catalogues (R2000 or C2013), and *TESS* measurements of the dominant pulsation mode. While the timescales of continuous *TESS* observations of our sample are too small to conduct a complete analysis of amplitude modulation, a

[3] https://github.com/jvines/astroARIADNE

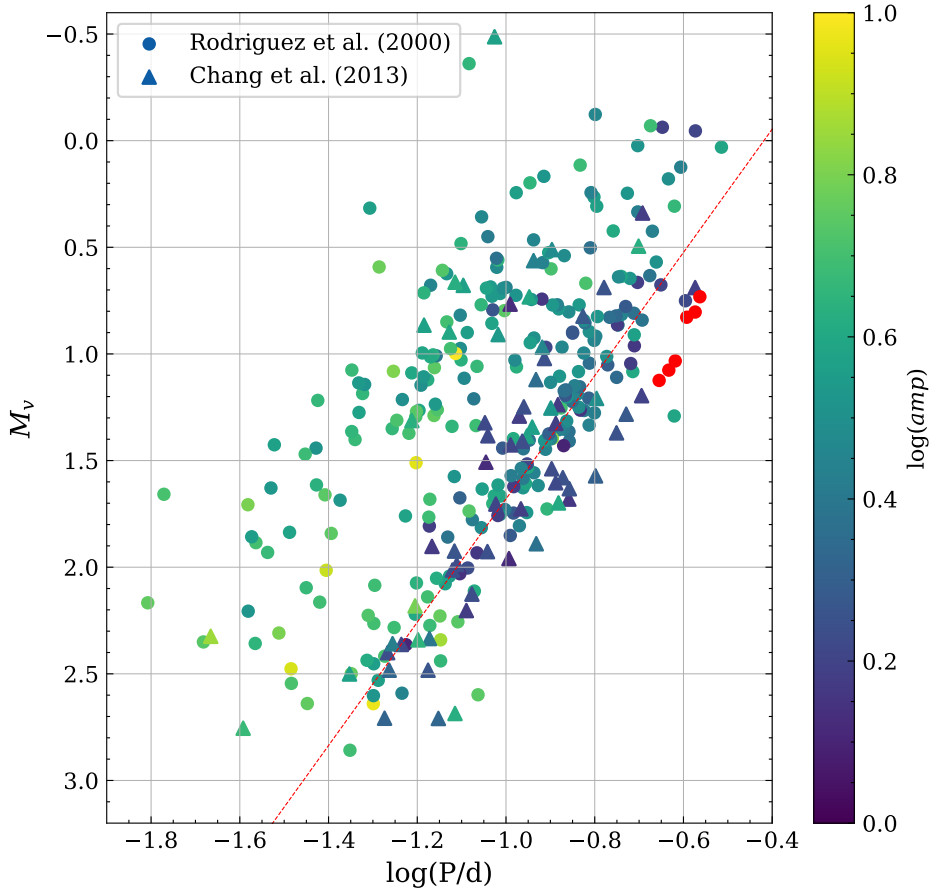

Figure 2. Period–luminosity diagram of δ Sct sample revised using data from the *TESS* mission. The stars plotted are restricted to variables having apparent V magnitudes brighter than 12.0 mag, and fractional parallax uncertainties less than 5 percent. The red dots indicate RR Lyrae variables.

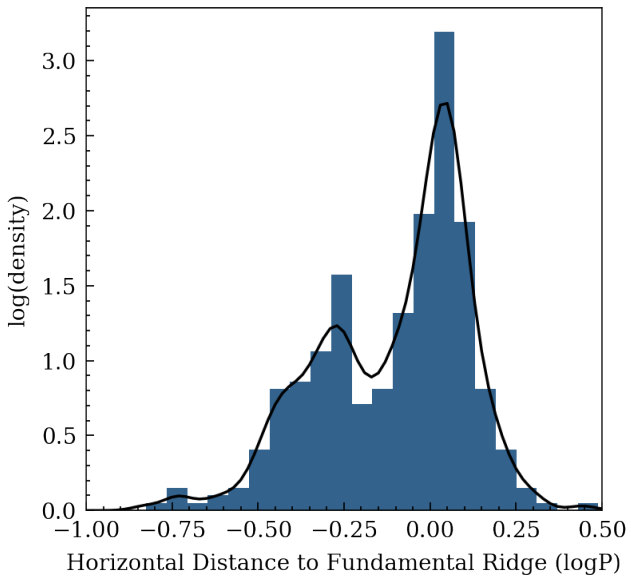

Figure 3. Histogram showing the horizontal distance of data points to the P–L relation calculated by Ziaali et al. (2019), overlaid with a fixed-bandwidth kernel density estimate (KDE; Terrell & Scott 1992) highlighting the same excess of stars displaced by −0.3 in log P from the fundamental mode ridge.

number of stars in our sample have *TESS* observations separated by a year or more. Interestingly, of these, several second ridge stars show modulation of the second-ridge mode between observations, so that the fundamental radial mode becomes the dominant mode.

IW Vel (HD 94985) is one such example. IW Vel was observed by *TESS* in Sector 10 in 2019, and again in Sectors 36 and 37 in 2021. Figure 5 shows clear amplitude modulation of the second ridge mode (10.15 d^{-1}) between Sectors 10 and 36, two years apart, continuing to Sector 37. In total, the amplitude drops by 67 percent between Sectors 10 and 37, with a 25 percent decrease occurring between Sectors 36 and 37. This moves IW Vel off the second ridge.

Similarly, BS Scl was observed by *TESS* in Sector 2 in 2018, and again in Sector 29 in 2020. In Sector 2, the second ridge mode at 17.63 d^{-1} is dominant with an amplitude of 1.38 ppt, while the fundamental radial mode peak at 8.83 d^{-1} has an amplitude of 1.29 ppt. By Sector 29 however, the second ridge mode has decreased in amplitude by 27 percent and is no longer the dominant frequency. We also note that the peak at 11.2 d^{-1} undergoes significant modulation, decreasing in amplitude by about 42 percent.

In summary, it is possible that stars occupy the second ridge only temporarily, perhaps when a mode of higher radial order is boosted to a higher amplitude through interactions with other modes.

Finally, we note that the amplitude spectrum of HQ Hya (Fig. 4) is similar to those of a new class of δ Sct stars that have been identified in *Kepler* data (see Fig. B12 of Murphy et al. 2019).

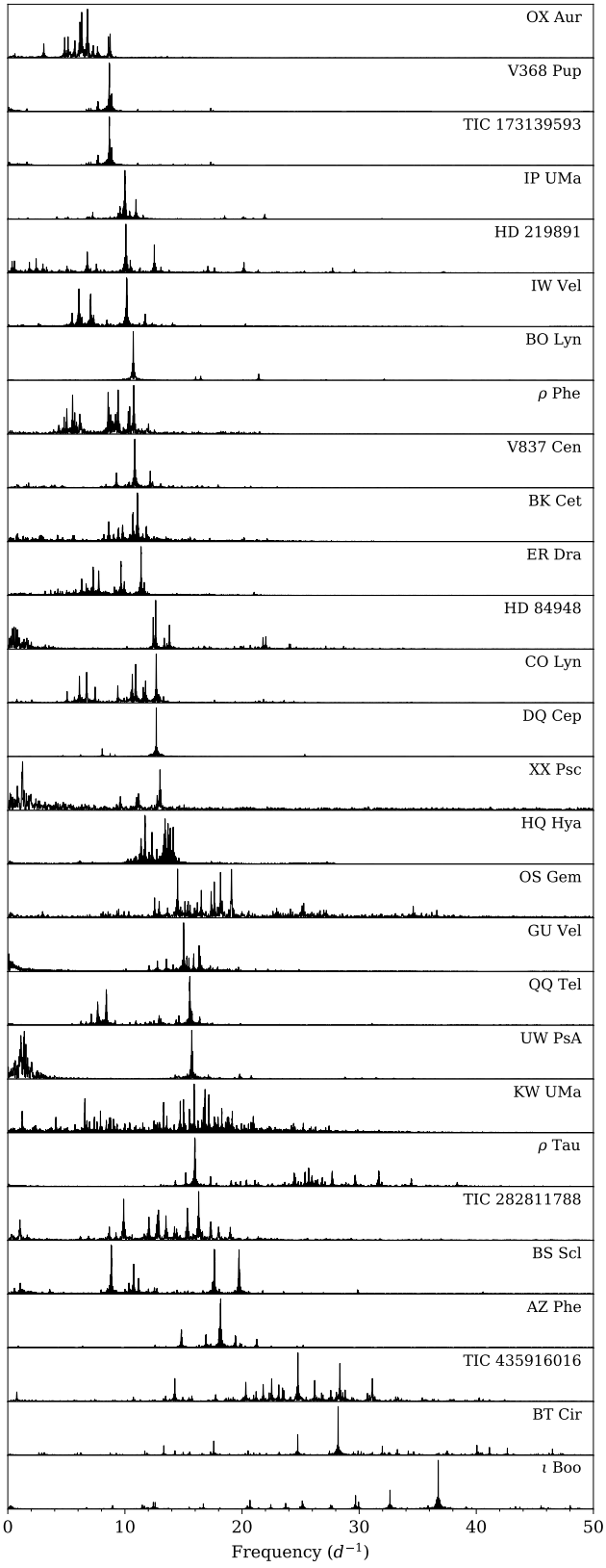

Figure 4. Pulsation spectra of the 28 δ Sct stars lying on the second ridge of our Period–Luminosity diagram, ordered by increasing frequency of the dominant pulsation mode. The vertical axis is amplitude in arbitrary units.

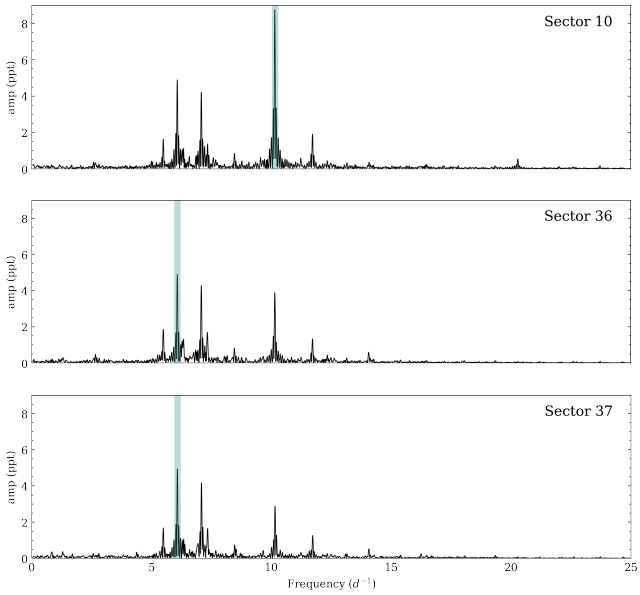

Figure 5. Pulsation spectra of IW Vel, a second ridge star, in Sectors 10, 36, and 37. The highlighted mode is the dominant mode.

These stars are characterised by a broad power excess containing many closely spaced peaks, rather than the more widely separated peaks that are seen in most δ Sct stars. We are not aware of an explanation of this phenomenon but we have noticed several other examples in our sample (e.g., BG Hyi, AI Scl, VV Ari and 60 Tau = V775 Tau).

4.2 Period–density relation of the *Kepler* δ Scuti sample

There have been numerous studies of the several thousand δ Sct stars observed by the *Kepler* Mission (for reviews, see Guzik 2021; Kurtz 2022). Here, we take advantage of the Gaia parallaxes to investigate their period–density relation. There is a well-established relationship between the period of a pulsating star and its mean density (e.g., Catelan & Smith 2015, sec. 5.2). The relation is usually written as

$$P = Q \left(\frac{\rho}{\rho_\odot} \right)^{-0.5} , \tag{4}$$

where the pulsation constant, Q, has a different value for each mode.[4] For the fundamental radial mode in δ Sct stars, Q is about 0.033 d (e.g., Fitch 1981; North et al. 1997; Breger 2000; Lovekin & Guzik 2017).

Calculating densities for a large number of stars requires estimating masses by fitting evolutionary tracks in the H–R diagram. This has been done using Gaia DR2 parallaxes for the full set of *Kepler* targets by Berger et al. (2020) and we used their masses and radii to estimate densities the *Kepler* δ Sct stars. Figure 6 show the period–density relation, where period of the dominant mode in each star was taken from Murphy et al. (2019). The diagram looks very similar to the period–luminosity relation (Ziaali et al. 2019)

[4] Note that Eq. 4 applies to pressure modes (p modes), which include pulsations in δ Scuti stars, β Cephei stars and solar-like oscillators. It does not apply to gravity modes (g modes), such as those in γ Doradus stars, Slowly Pulsating B stars and white dwarfs.

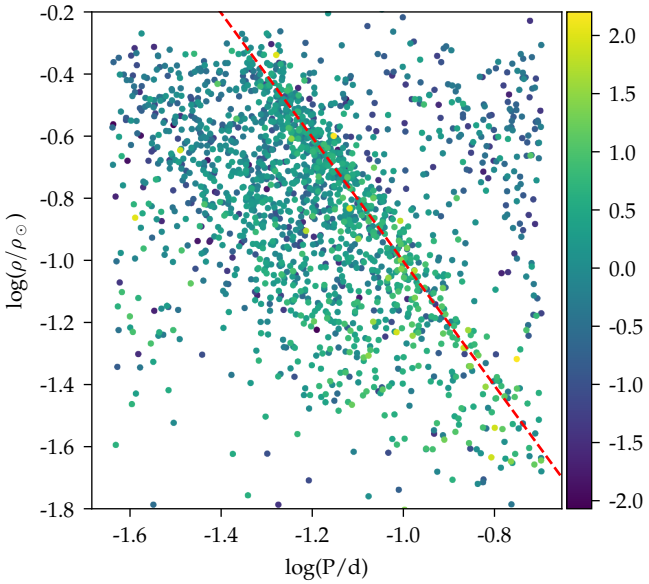

Figure 6. Period–density relation for *Kepler* δ Sct stars. Points show the dominant pulsation mode in each star, colour-coded by the logarithm of the pulsation amplitude in ppt. Pulsation periods and amplitudes were taken from Murphy et al. (2019) and densities were calculated from the *Kepler Stellar Properties Catalog* (Berger et al. 2020). The red dashed line shows the theoretical period–density relation (Eq. 4) with a pulsation constant of $Q = 0.0315$ d. Points in the upper right are γ Dor stars (see Ziaali et al. 2019).

but with the vertical axis reversed, which is expected because of the tight inverse correlation between luminosity and density. Most points in Fig. 6 lie on a ridge that corresponds to the radial fundamental mode. This is confirmed by the dashed line, which shows the theoretical relation (Eq. 4) with $Q = 0.0315$ d. We also see clearly the excess of points on the second ridge, with half this period.

5 HIGH-FREQUENCY δ SCUTI STARS

Some of the stars in our sample belong to the class of high-frequency δ Sct stars, discovered by Bedding et al. (2020) to have remarkably regular sequences of overtone modes. Three were listed in that paper, namely EX Eri (HD 30422), V435 Car (HD 44958) and V349 Pup (HD 59594), but only for V435 Car was the échelle diagram shown. The échelle diagram for EX Eri was shown by Murphy et al. (2020), who also showed échelle diagrams for four other stars in our sample: V1023 Cen (HD 102541), MO Hya (HD 111786), V346 Pav (HD 168740) and HD 210111. It is noteworthy that in high-frequency δ Sct stars stars, the fundamental mode is rarely the strongest mode. We show two examples here.

5.1 XX Pyx

XX Pyx is a multi-periodic pulsator that has been the subject of three ground-based multi-site campaigns (Handler et al. 2000, and references therein). The star was not observed by *TESS* in Cycle 1 because it fell in a gap between fields, but it was observed in Cycle 3 (Sector 35). The *TESS* light curve (Fig. 7) confirms that it is an ellipsoidal variable with a binary period of 1.15 d, as found by Aerts et al. (2002).

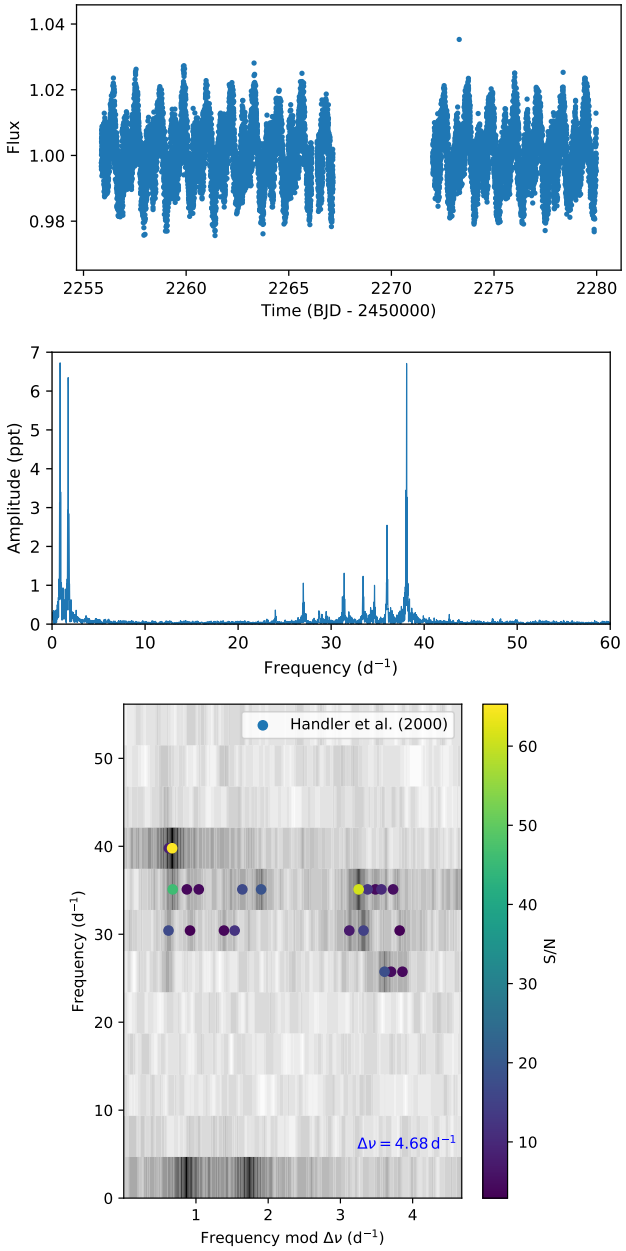

Figure 7. *TESS* observations of XX Pyx (Sector 35), showing the light curve (top), the amplitude spectrum (middle), and the amplitude spectrum in échelle format. The circles in the échelle diagram show the frequencies reported by Handler et al. (2000), colour-coded by signal-to-noise (their Table 4).

Handler et al. (2000) detected 19 independent pulsation frequencies in the range 27–38 d^{-1}, and suggested a large separation of 4.63 d^{-1}. By generating an échelle diagram with those frequencies, Bedding et al. (2020) confirmed that a value of $\Delta\nu = 4.70\,d^{-1}$ gave a reasonably good alignment of the peaks. Figure 7 shows the *TESS* amplitude spectrum in échelle format. We confirm that $\Delta\nu = 4.68\,d^{-1}$ produces a ridge on the left-hand-side that we can identify as $l = 1$ modes (see Bedding et al. 2020 for discussion of similar stars). Three of these modes were detected by Handler et al. (2000), and we see two additional weaker $l = 1$ modes in this ridge. This star is clearly worthy of further study.

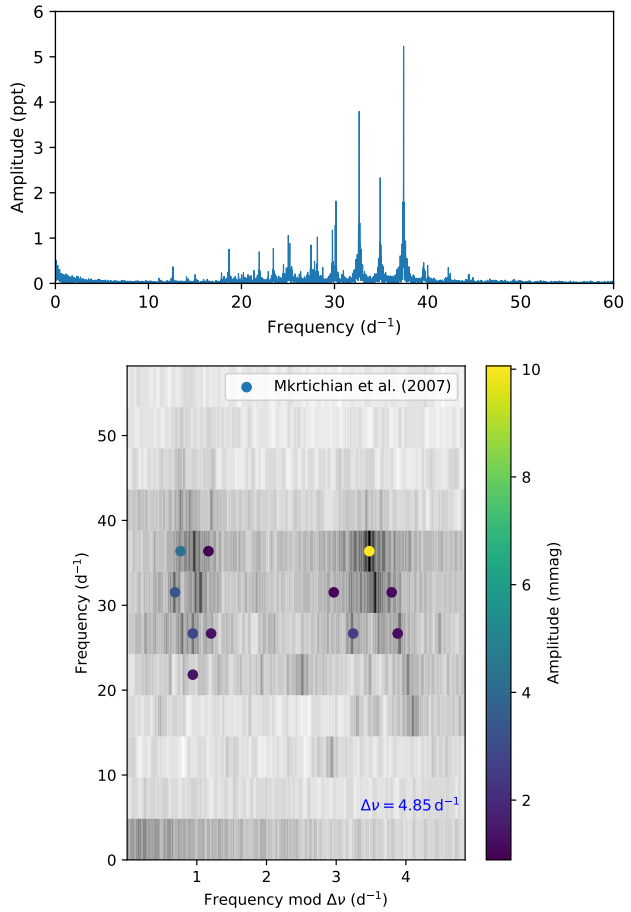

Figure 8. *TESS* observations of 29 Cyg (Sectors 14 and 15), showing the amplitude spectrum (top), and the échelle diagram (bottom). The circles show the frequencies reported by Mkrtichian et al. (2007), colour-coded by amplitude (their Table 8).

5.2 29 Cyg

29 Cyg (V1644 Cyg; HD 192640) is a multi-periodic pulsator that has been the subject of two ground-based multi-site campaigns by Mkrtichian et al. (2007). They measured 11 modes in the range 20–37 d^{-1} and suggested a large separation of $\Delta\nu = 4.82$ d^{-1}. Theoretical models using these frequencies were calculated by Casas et al. (2009). The *TESS* data, shown in Fig. 8, confirm that 29 Cyg is a high-frequency δ Sct star with a large separation of $\Delta\nu = 4.85$ d^{-1}. With a magnitude of $V = 4.9$, this makes 29 Cyg the brightest known member of this class of stars and an ideal target for follow-up observations. It is also known to be a λ Boo star, which is common among high-frequency δ Sct stars (Bedding et al. 2020; Murphy et al. 2020).

6 CONCLUSIONS

We have examined 488 stars observed by the *TESS* mission, drawn from the R2000 and C2013 catalogues of δ Sct stars. For each target, we have redetermined their strongest peak from the *TESS* light curve, thus revising our sample to provide more precise and homogeneous measurements of the dominant pulsation modes using *TESS* data, ultimately identifying 54 stars as showing no evidence of δ Sct pulsations. Using the remaining targets and their revised data, we have revisited the period–luminosity relationship of δ Sct stars, and demonstrated its value in helping to identify stars which have been misclassified as δ Sct pulsators.

We have investigated an excess of stars forming a sharp second ridge in the period-luminosity diagram, first identified by Ziaali et al. (2019). This ridge is displaced by −0.3 in log P, corresponding to a period ratio of 0.5. Given that several stars falling on this ridge undergo amplitude modulation of the second-ridge peak on timescales of years, this may signify energy transfer between modes and suggests a transient nature to a star's occupation of the second ridge. Finally, we identified several high-frequency δ Sct stars, including XX Pyx and 29 Cyg.

ACKNOWLEDGEMENTS

We gratefully acknowledge support from the Australian Research Council through DECRA grant DE180101104, Future Fellowship FT210100485, and Discovery Project DP210103119, and from the Danish National Research Foundation (Grant DNRF106) through its funding for the Stellar Astrophysics Center (SAC). This work has made use of data from the European Space Agency (ESA) mission *Gaia*, (`https://www.cosmos.esa.int/gaia`), processed by the *Gaia* Data Processing and Analysis Consortium (DPAC, `https://www.cosmos.esa.int/web/gaia/dpac/consortium`). Funding for the DPAC has been provided by national institutions, in particular the institutions participating in the *Gaia* Multilateral Agreement. We are grateful to the entire Gaia and *Kepler* teams for providing the data used in this paper. We also thank László Molnár for useful discussions on RR Lyrae stars.

REFERENCES

Aerts C., 2021, Reviews of Modern Physics, 93, 015001
Aerts C., Handler G., Arentoft T., Vandenbussche B., Medupe R., Sterken C., 2002, MNRAS, 333, L35
Antonello E., Pasinetti Fracassini L. E., 1998, A&A, 331, 995
Bedding T. R., et al., 2020, Nature, 581, 147
Berger T. A., Huber D., van Saders J. L., Gaidos E., Tayar J., Kraus A. L., 2020, AJ, 159, 280
Bowman D. M., Kurtz D. W., Breger M., Murphy S. J., Holdsworth D. L., 2016, MNRAS, 460, 1970
Breger M., 2000, in ASP Conf. Series, Vol. 210. p. 3
Casas R., Moya A., Suárez J. C., Martín-Ruíz S., Amado P. J., Rodríguez-López C., Garrido R., 2009, ApJ, 697, 522
Castelli F., Kurucz R. L., 2003, in Piskunov N., Weiss W. W., Gray D. F., eds, IAU Symposium Vol. 210, Modelling of Stellar Atmospheres. p. A20 (`arXiv:astro-ph/0405087`)
Catelan M., Smith H. A., 2015, Pulsating Stars. Wiley-VCH
Chang S. W., Protopapas P., Kim D. W., Byun Y. I., 2013, AJ, 145, 132
ESA 1997, The HIPPARCOS and TYCHO catalogues. Astrometric and photometric star catalogues derived from the ESA HIPPARCOS Space Astrometry Mission. ESA Special Publication Vol. 1200, ESA Publications Division, Noordwijk, Netherlands
Fitch W. S., 1981, ApJ, 249, 218
Garofalo A., Delgado H. E., Sarro L. M., Clementini G., Muraveva T., Marconi M., Ripepi V., 2022, arXiv e-prints, p. arXiv:2203.07435
Guzik J. A., 2021, Frontiers in Astronomy and Space Sciences, 8, 55
Handler G., et al., 2000, MNRAS, 318, 511
Huber D., et al., 2010, ApJ, 723, 1607
Jayasinghe T., et al., 2020, MNRAS, 493, 4186
Kurtz D., 2022, arXiv e-prints, p. arXiv:2201.11629

Leavitt H. S., Pickering E. C., 1912, Harvard College Observatory Circular, 173, 1
Li L.-J., Qian S.-B., Zhang J., Zhu L.-Y., Liao W.-P., 2018, Research in Astronomy and Astrophysics, 18, 011
Liakos A., Niarchos P., 2017, MNRAS, 465, 1181
Lightkurve Collaboration et al., 2018, Lightkurve: Kepler and TESS time series analysis in Python, Astrophysics Source Code Library (ascl:1812.013)
Lovekin C. C., Guzik J. A., 2017, ApJ, 849, 38
McNamara D. H., 2011, AJ, 142, 110
Mkrtichian D. E., et al., 2007, AJ, 134, 1713
Molnár L., et al., 2022, ApJS, 258, 8
Murphy S. J., 2012, MNRAS, 422, 665
Murphy S. J., Hey D., Van Reeth T., Bedding T. R., 2019, MNRAS, 485, 2380
Murphy S. J., Paunzen E., Bedding T. R., Walczak P., Huber D., 2020, MNRAS, 495, 1888
North P., Jaschek C., Egret D., 1997, in Bonnet R. M., et al., eds, ESA Special Publication Vol. 402, Hipparcos – Venice '97. p. 367
Ochsenbein F., Bauer P., Marcout J., 2000, A&AS, 143, 23
Pigulski A., Pojmański G., 2008, A&A, 477, 907
Poro A., et al., 2021, PASP, 133, 084201
Rodríguez E., López-González M. J., López de Coca P., 2000, A&AS, 144, 469
Sneden C., et al., 2018, AJ, 155, 45
Speagle J. S., 2020, MNRAS, 493, 3132
Steindl T., Zwintz K., Bowman D. M., 2021, A&A, 645, A119
Terrell G. R., Scott D. W., 1992, The Annals of Statistics, 20, 1236
Ziaali E., Bedding T. R., Murphy S. J., Van Reeth T., Hey D. R., 2019, MNRAS, 486, 4348

Table 1: Properties of δ Sct stars.

HD	Name	TIC	f_{cat} d^{-1}	f_1 d^{-1}	a_1 ppt	dist pc	e_dist pc	A_v mag	e_A_v mag	M_v mag
205		359127550		6.25	8.40	307.96	1.16	0.10	0.06	1.21
1097	AU Scl	12473170	17.73	16.55	1.54	325.34	5.44	0.13	0.05	1.37
2628	GN And	440665786	14.43	14.43	5.83	61.23	0.54	0.05	0.04	1.24
2724	BB Phe	116157537	5.74	5.73	3.30	134.51	0.38	0.11	0.05	0.42
3112	θ Tuc	38847248	20.28	20.28	4.90	139.98	0.44	0.07	0.05	0.32
3326	BG Cet	98660068	33.44	30.52	0.21	50.66	0.09	0.06	0.03	2.48
4490	XX Psc	435860104	9.62	12.99	0.13	102.20	0.28	0.06	0.04	1.00
4494	CN Phe	80432574	14.29	12.84	1.12	266.09	1.22	0.07	0.03	2.26
4849	AZ Phe	80474886	18.15	18.05	2.04	97.06	0.63	0.20	0.07	1.35
4919	ρ Phe	369666165	5.45	10.75	5.99	75.00	0.29	0.13	0.10	0.73
6667		248345301	18.02	18.02	14.65	255.76	6.46	0.06	0.05	2.36
6870	BS Tuc	234548714	15.38	17.87	1.72	107.55	0.19	0.04	0.03	2.28
7312	AI Scl	183595451	24.04	10.71	2.48	68.68	0.11	0.06	0.04	1.70
8511	AV Cet	10838265	14.60	15.91	2.57	66.25	0.13	0.04	0.03	2.07
8781	BG Hyi	52258534	8.96	9.04	3.98	186.10	0.47	0.11	0.05	1.61
9065	WZ Scl	70489756	10.43	10.42	4.93	93.51	0.21	0.12	0.04	1.61
9100	VX Psc	381320713	7.35	6.34	5.15	138.79	0.61	0.05	0.04	0.26
9133	XX Scl	70490868	20.45	21.45	4.27	334.22	6.03	0.02	0.02	1.27
9800	V0365 And	308719469	7.00	7.00	14.12	168.37	0.53	0.11	0.07	1.15
11285	VV Ari	91277922	13.09	12.63	2.49	168.27	1.07	0.10	0.05	0.48
11413	BD Phe	229150702	26.81	26.80	7.78	78.04	0.17	0.03	0.03	1.44
11522	BK Cet	92984630	11.07	11.07	4.17	101.36	0.32	0.07	0.04	0.69
11667		229154157	10.99	10.99	82.16	457.77	2.32	0.06	0.05	1.38
11956	FG Eri	231048083	6.29	6.29	11.23	230.32	0.91	0.03	0.02	-0.12
12389		63395663	25.00	20.83	7.04	229.70	2.23	0.03	0.03	1.14
12743	V0373 And	184589181	8.87	9.24	12.85	153.77	0.49	0.10	0.05	1.54
13079	V0419 And	184679514	20.00	19.41	4.91	181.74	0.64	0.08	0.06	2.53
13122	V0784 Cas	12221925	9.16	9.16	16.45	98.18	0.27	0.10	0.06	1.58
13755	CV Phe	7245720	12.50	7.92	6.61	200.20	0.65	0.08	0.05	1.25
15634	TY For	120932152	10.30	10.29	3.97	91.93	0.85	0.04	0.04	1.67
16189	DX Cet	278962831	9.62	9.62	52.91	109.16	0.32	0.07	0.06	1.75
16439	V0663 Cas	280129361	17.12	17.13	8.64	309.04	1.52	0.03	0.02	1.21
16698	FI Eri	142266756	5.84	5.84	26.44	324.29	3.10	0.08	0.05	0.83
16723	BS Cet	441131892	8.93	7.61	6.30	147.60	0.50	0.07	0.05	0.79
17138	RZ Cas	302771290	64.10	64.20	0.98	65.31	0.10	0.03	0.02	2.17
17978	VV For	65484200	17.33	11.79	3.21	324.82	1.89	0.05	0.04	2.11
18655		365225836	14.88	14.88	19.55	283.54	1.74	0.07	0.05	2.33
18878	V0509 Per	192374290	6.86	6.86	6.45	115.94	0.35	0.07	0.04	1.08
19279	V0521 Per	192533869	14.45	14.85	1.61	86.13	0.25	0.02	0.02	1.68
20313	BN Hyi	348762920	15.15	17.94	0.64	80.27	0.28	0.07	0.05	1.08
20429	AR Ari	28833184	5.65	5.15	24.35	239.09	2.01	0.11	0.09	0.81
20919	V0461 Per	252829836	28.57	28.04	0.97	181.26	1.07	0.09	0.04	2.64
21190	CP Oct	348772511	6.68	6.68	11.30	200.14	2.48	0.13	0.07	1.00
21553	V0465 Per	347570557	14.04	14.04	2.14	180.75	0.61	0.04	0.03	2.44
22541	AD Hor	79611815	10.99	10.99	16.73	203.79	0.76	0.03	0.02	0.45
23728	V0376 Per	432049507	10.06	10.06	20.09	67.90	0.77	0.08	0.07	1.73
24550	V0479 Tau	459908110	13.19	13.24	2.28	152.57	0.44	0.17	0.06	1.34
24809	V0386 Per	94549636	18.18	22.32	0.92	63.84	0.09	0.01	0.01	2.50
26574	omi 1 Eri	67687505	13.39	12.23	5.29	38.42	0.22	0.22	0.17	0.90
26892	UZ Ret	38515566	8.14	8.14	12.72	339.81	1.18	0.12	0.06	1.45
27093	IU Eri	67781014	14.51	12.48	4.56	226.69	1.08	0.03	0.02	0.68
27397	V0483 Tau	435910664	18.21	20.45	1.25	45.48	0.11	0.06	0.05	2.23
27459	V0696 Tau	435916016		24.77	1.05	47.40	0.24	0.03	0.03	1.84
27503	BR Hyi	25195864	5.00	26.74	2.61	664.38	4.97	0.06	0.05	1.61
27545	TX Ret	38587180	14.93	9.63	3.19	199.33	0.54	0.07	0.04	1.40
27628	V0775 Tau	435923755	15.87	14.04	0.41	45.42	0.14	0.09	0.05	2.34
28052	V0777 Tau	60879864	5.49	5.18	3.43	46.72	0.48	0.05	0.04	1.08
28665	EQ Eri	178880326	14.29	14.37	17.21	212.39	0.83	0.08	0.05	1.01

Table 1 — continued from previous page

HD	Name	TIC	f_{cat} d^{-1}	f_1 d^{-1}	a_1 ppt	dist pc	e_dist pc	A_v mag	e_A_v mag	M_v mag
28837	RX Cae	7808834	6.49	6.49	26.72	147.51	1.36	0.13	0.08	1.04
28910	ρ Tau	245860427	14.93	15.97	1.39	46.31	0.29	0.03	0.03	1.29
30600	HV Eri	167486272	4.74	4.74	21.82	339.75	2.59	0.06	0.05	0.63
30716	V1359 Ori	11083205	5.49	5.49	12.47	323.51	3.90	0.10	0.06	0.82
32045	S Eri	152373997	3.66	3.27	3.94	86.75	0.60	0.06	0.05	0.03
32846	X Cae	77669416	7.40	7.39	24.18	104.70	0.57	0.05	0.05	1.17
33959	KW Aur	1840666	11.35	11.35	10.82	83.24	0.72	0.05	0.05	0.36
34409	BS Cam	417652271	5.54	4.17	2.05	401.04	2.87	0.11	0.06	0.31
37857	EE Cam	70657495	4.93	4.93	20.85	223.94	0.88	0.11	0.09	0.84
38882	RY Lep	93441696	4.44	4.44	103.12	437.06	15.66	0.13	0.11	-0.06
39244	YY Pic	299884840	9.74	9.74	16.01	153.22	0.36	0.04	0.03	1.57
39996	AA Col	100830119	6.66	6.66	16.79	226.17	0.80	0.11	0.07	1.27
40372	V1004 Ori	282270717	16.39	15.31	2.49	106.63	0.37	0.04	0.03	0.71
40535	V0474 Mon	67265166	7.35	7.34	54.70	93.82	0.26	0.09	0.07	1.19
40765	UY Col	143168754	5.90	5.90	42.79	474.20	2.46	0.12	0.09	1.05
44958	V0435 Car	255548143	20.00	20.57	3.14	71.29	0.08	0.03	0.03	2.44
45311	V0456 Aur	144101735	7.21	7.21	22.64	187.98	1.41	0.11	0.07	1.36
50018	OX Aur	21291018	6.46	6.81	1.78	147.78	0.93	0.15	0.07	0.11
50420	V0352 Aur	191999705	5.88	3.76	1.74	298.10	2.92	0.12	0.07	-1.33
52788	V0383 Car	279361762	8.33	10.76	4.22	303.99	1.08	0.14	0.07	0.86
55057	V0571 Mon	5456605	10.00	5.25	6.68	87.49	0.49	0.08	0.05	0.65
55595	HN CMa	65472324	4.00	4.72	1.67	211.84	0.86	0.04	0.02	-0.07
58634	V0368 Pup	173139593	8.67	8.67	13.40	180.87	0.57	0.02	0.02	0.56
58634	V0368 Pup	173139598	8.67	8.67	11.78	181.72	0.53	0.06	0.04	0.47
58954	NR CMa	49832986	6.02	6.84	5.93	89.97	0.27	0.09	0.05	0.77
59594	V0349 Pup	112484997	19.88	19.87	5.14	93.34	0.16	0.02	0.02	2.45
60302	V0344 Gem	247165103	8.46	8.46	9.06	185.60	0.81	0.07	0.04	1.62
62437	AZ CMi	280680714	10.49	10.51	22.84	148.81	1.09	0.05	0.03	0.55
63874		39011225	5.42	13.03	2.82	213.93	8.51	0.09	0.05	0.66
64191	AD CMi	266328148	8.13	8.13	85.70	451.67	2.90	0.08	0.06	0.97
64491	DD Lyn	14878438	20.41	19.76	1.69	64.93	0.32	0.08	0.04	2.08
66260	V0393 Car	364399376	7.14	7.08	56.51	199.66	3.54	0.07	0.05	0.90
67028		452926063	19.31	19.32	0.83	431.76	4.37	0.05	0.03	0.59
67147	CO Lyn	80951366	6.11	12.67	8.74	141.61	0.39	0.10	0.06	0.97
67290	V0355 Pup	176152984	6.71	9.48	4.90	368.17	2.65	0.05	0.03	0.24
67390	SZ Lyn	192939152	8.30	8.30	138.77	525.06	25.47	0.10	0.09	0.74
67523	ρ Pup	154360594	7.10	7.10	24.63	19.44	0.08	0.13	0.12	1.22
67911	CQ Lyn	81003138	8.87	8.86	22.32	196.57	1.57	0.10	0.07	1.40
69213	AI Vel	81709032	8.96	8.96	90.13	100.30	0.17	0.05	0.05	1.52
69242	CR Lyn	22684612	7.59	7.59	12.84	172.91	0.65	0.10	0.07	1.36
69997	HQ Hya	19566581	13.25	13.33	1.61	110.32	0.24	0.12	0.05	0.98
71297	LM Hya	169051549	26.32	26.29	1.63	46.74	1.25	0.09	0.14	2.16
71935	GU Vel	140349824	14.29	15.01	2.96	60.66	0.27	0.04	0.04	1.12
73857	VZ Cnc	366632312	5.61	5.61	120.42	221.97	1.15	0.11	0.07	0.86
74292	FL Cnc	165859518	12.50	13.41	4.79	97.47	0.25	0.05	0.03	2.04
75654	HZ Vel	190158777	11.49	14.34	3.03	71.85	0.09	0.04	0.03	2.05
77906		401744720	12.90	12.91	73.66	344.85	7.24	0.09	0.06	1.99
78422	NT Hya	20042408	6.94	6.91	12.38	165.86	0.59	0.09	0.06	1.19
79185	MP Vel	74528796	4.29	7.92	1.47	269.47	1.13	0.10	0.05	0.60
79439	DD UMa	137648019	8.00	25.43	0.26	35.83	0.10	0.03	0.02	2.01
79781	GG UMa	86232782	7.42	7.42	16.17	266.90	1.00	0.12	0.07	1.35
79889	BE Lyn	56914404	10.43	10.43	110.06	251.63	1.31	0.04	0.04	1.76
81882	KZ UMa	147893556	16.67	14.28	1.32	229.55	0.97	0.06	0.04	1.26
82620	DL UMa	147574768	12.03	13.08	6.94	126.72	0.26	0.10	0.04	1.57
83041	AK Ant	189569123	15.15	14.53	0.99	305.90	2.22	0.08	0.04	1.29
84712	MT Vel	34156938	12.50	13.60	6.64	240.74	1.50	0.08	0.04	0.62
84800	IX UMa	23969903	41.67	36.62	1.53	147.98	0.43	0.05	0.03	1.88
84948		453432481	12.82	12.63	2.65	255.19	3.95	0.06	0.04	1.03
84999	ups UMa	331900366	7.54	6.28	12.01	35.67	0.24	0.09	0.08	0.92

Table 1 — continued from previous page

HD	Name	TIC	f_{cat} d^{-1}	f_1 d^{-1}	a_1 ppt	dist pc	e_dist pc	A_v mag	e_A_v mag	M_v mag
85040	DG Leo	88024537	12.11	12.11	2.25	216.27	22.95	0.03	0.03	-0.36
86301	BF Ant	22234795		5.03	2.88	143.91	0.47	0.03	0.02	0.49
87700	V0336 Vel	462426434	8.27	12.42	10.70	132.24	0.26	0.13	0.06	1.11
88824	LW Vel	259761784	7.98	8.98	6.67	49.67	0.13	0.05	0.04	1.74
89343	EN UMa	103692670	9.09	6.43	12.82	130.07	0.69	0.06	0.04	0.24
90001	V0344 Vel	220628281	6.68	6.68	9.65	247.53	1.20	0.08	0.05	0.84
93044	EO UMa	17329905	11.90	11.91	15.86	113.97	0.28	0.06	0.04	1.78
93137	UX LMi	337319844	6.64	6.64	21.97	426.41	10.83	0.11	0.08	0.85
93142	AZ Ant	54253999	9.50	9.49	7.10	256.99	1.41	0.10	0.05	0.73
93298	V0353 Vel	106886169	4.04	4.04	14.48	312.77	1.88	0.04	0.03	0.12
94033	KZ Hya	188209486	16.81	16.80	222.64	330.80	7.19	0.11	0.09	2.36
94480	WW LMi	138738145		7.88	9.80	130.68	0.55	0.10	0.05	0.51
94985	IW Vel	120856811	6.67	10.15	8.75	108.68	0.26	0.03	0.02	0.69
95321	V0527 Car	304050480	4.68	4.68	14.61	531.78	6.11	0.05	0.05	0.42
97302	FI UMa	302349701	25.00	15.95	0.19	104.91	0.22	0.01	0.01	1.51
98851	LR UMa	144311964	18.15	8.97	4.04	152.44	0.54	0.12	0.06	1.38
99002	CX UMa	17992601	10.00	14.80	3.33	148.40	0.54	0.07	0.05	1.01
99983	HQ UMa	284596378	8.65	8.65	7.93	163.82	1.36	0.11	0.05	0.93
100363	SU Crt	157787615	18.18	18.77	1.51	169.76	1.65	0.05	0.04	2.42
101158	V0837 Cen	429143728	12.17	10.83	5.63	191.91	0.59	0.06	0.04	0.69
101696	VY Crt	270265624	7.34	7.34	27.62	131.88	2.89	0.12	0.08	1.17
102355	KW UMa	138590902	8.20	15.91	1.10	109.20	0.61	0.12	0.05	1.27
102541	V1023 Cen	454109915	20.00	19.90	6.75	115.78	0.31	0.03	0.02	2.60
104036	EE Cha	454961439	33.33	33.87	6.41	104.82	0.26	0.01	0.01	1.63
104288		142946146	8.87	8.86	3.67	206.93	17.00	0.10	0.06	0.73
105513	CO Cru	67533256	6.85	6.85	9.42	380.94	1.56	0.10	0.06	1.25
105759	II Vir	176867792	23.64	23.66	6.23	92.69	0.27	0.03	0.02	1.69
107131	FM Com	328860893	15.08	14.93	1.77	85.52	0.20	0.01	0.01	1.77
107513	KU Com	356702180	33.33	19.91	0.16	86.51	0.30	0.04	0.04	2.64
107904	AI CVn	284593009	8.60	5.05	15.33	131.81	1.32	0.10	0.07	0.33
109585	TU Crv	83207850	12.20	10.63	3.42	75.16	1.60	0.14	0.05	1.67
110377	GG Vir	390607729	20.00	34.46	1.91	71.65	0.16	0.01	0.01	1.93
110951	FM Vir	390633441	13.91	13.91	1.22	80.45	0.70	0.08	0.06	0.61
113537	V0947 Cen	453750774	7.29	7.30	9.04	99.95	0.28	0.12	0.07	1.31
114042	V0950 Cen	253513495	6.61	6.61	1.37	258.12	1.66	0.04	0.02	0.67
114620	V0954 Cen	442837381	9.14	9.14	19.95	139.80	0.31	0.09	0.07	1.44
115308	DK Vir	66693422	8.61	7.58	6.66	125.16	0.38	0.10	0.05	1.10
115604	AO CVn	180651551	8.22	8.22	6.58	78.25	0.64	0.07	0.07	0.17
116994	V0743 Cen	438816206	9.78	9.78	50.85	226.64	1.08	0.07	0.06	1.85
117661	HX Vir	32146574	23.26	22.27	2.23	83.08	0.22	0.04	0.03	1.36
118326	LW Mus	342500794	6.51	6.51	36.48	375.31	8.82	0.14	0.09	1.21
118743	BZ Boo	282811788	2.70	16.30	2.68	225.58	1.73	0.10	0.04	1.31
118954	IP UMa	458452969	10.00	10.00	13.76	240.65	0.97	0.08	0.04	0.69
120500	FQ Boo	399182167	20.41	21.05	2.22	120.91	0.64	0.01	0.01	1.19
120896	QT Vir	392979958	17.79	7.62	3.34	223.10	0.98	0.07	0.04	1.70
121517		241787384	9.01	11.01	67.64	300.62	1.26	0.09	0.08	1.93
123460		242302902	7.64	7.64	121.86	644.85	8.39	0.10	0.10	1.24
124675	κ Boo	310362802	15.43	15.44	3.96	49.63	0.21	0.04	0.03	1.00
124953	CN Boo	135169898	22.83	11.56	1.08	46.20	0.06	0.04	0.03	2.60
125081	MX Vir	46041110	6.49	6.50	12.89	149.23	0.44	0.15	0.10	1.33
125161	ι Boo	310381204	37.74	36.75	2.35	29.51	0.06	0.03	0.03	2.36
125162	λ Boo	168708816	43.48	38.17	0.68	30.64	0.12	0.03	0.03	1.71
126859	V0853 Cen	290932786	18.94	16.31	3.58	140.57	0.25	0.15	0.04	1.09
127269	MP Hya	83860356	29.94	28.36	1.82	180.57	0.97	0.03	0.02	1.47
127411	IT Dra	166177270	23.04	16.85	4.23	139.30	0.32	0.04	0.03	1.76
127695	V1034 Cen	395108754	4.26	4.18	3.88	282.55	1.01	0.13	0.06	1.29
127711	V1035 Cen	395425079	12.50	11.68	1.73	276.62	2.37	0.16	0.04	1.34
127759	EI Dra	166179291	14.79	14.79	11.66	365.20	1.82	0.05	0.03	0.68
127762	gam Boo	67991192	13.70	13.59	1.60	26.29	0.12	0.07	0.05	0.85

Table 1 — continued from previous page

HD	Name	TIC	f_{cat} d^{-1}	f_1 d^{-1}	a_1 ppt	dist pc	e_dist pc	A_v mag	e_A_v mag	M_v mag
127929	ER Dra	166179517	11.35	11.38	2.29	122.26	0.33	0.07	0.03	0.77
128157	V0896 Cen	430665759	20.00	19.86	1.61	152.75	0.46	0.11	0.05	2.26
128862	PR Aps	402305954		10.42	6.01	251.40	1.05	0.13	0.06	0.91
129041	BT Cir	403779926	28.25	28.20	2.00	114.10	0.27	0.03	0.02	2.10
129494	BO Cir	292435853	7.08	8.08	2.25	364.32	1.63	0.18	0.08	1.73
132209	BV Cir	453848870	6.33	6.33	11.93	127.77	0.30	0.10	0.05	0.94
133194	HY Lib	440958702	6.82	6.82	25.62	194.10	1.01	0.13	0.09	1.15
134185	HU Lup	122932611	6.52	7.66	13.01	454.35	2.64	0.11	0.07	0.77
135383	OP Aps	407012535	7.20	7.20	21.83	207.83	0.71	0.09	0.07	1.41
140639		178463456	4.95	4.95	100.97	425.87	2.98	0.15	0.12	1.20
143466	CL Dra	458485558	13.11	14.85	1.78	33.78	0.08	0.05	0.04	2.27
148638	NP TrA	402646773	16.31	15.30	4.65	251.30	1.35	0.03	0.02	0.87
149530	V1060 Sco	280816457	5.53	5.58	9.32	404.33	2.83	0.15	0.09	0.64
153747	V0922 Sco	346505765	21.28	21.47	5.77	177.14	0.69	0.04	0.03	1.14
153805	V1072 Sco	347028423	7.47	7.48	11.13	182.73	1.09	0.09	0.05	0.97
154605		43173526	9.93	11.94	75.50	285.17	1.18	0.19	0.12	2.13
155118	V0873 Her	143166570	7.91	7.86	0.52	240.52	1.61	0.10	0.07	1.40
155514	V0620 Her	257456864	11.31	11.32	5.08	80.12	0.11	0.04	0.04	1.63
159223	V0648 Her	321813050	3.45	46.30	0.43	79.24	0.10	0.03	0.03	2.32
161032	V0352 Pav	306889170	9.35	11.82	18.18	110.58	0.29	0.08	0.05	1.21
161287	V0966 Her	256007029	7.52	7.52	1.60	212.82	0.69	0.09	0.06	1.25
168740	V0346 Pav	365996589	27.78	30.75	4.24	71.12	0.14	0.03	0.02	1.84
168947	V0704 CrA	89975166	17.24	14.60	2.88	258.05	1.64	0.06	0.04	1.00
170625	V0668 CrA	91406903	11.36	26.56	2.05	298.55	1.41	0.12	0.06	1.22
173844		359678383	15.80	15.78	2.35	178.29	0.36	0.05	0.03	2.34
173977	HN Dra	232637376	8.56	8.56	27.46	236.28	0.86	0.09	0.07	1.12
176503	V0544 Lyr	20816780	8.83	8.83	2.37	271.50	1.20	0.07	0.04	0.20
176723	V0701 CrA	254079940	7.39	8.94	3.55	65.38	0.21	0.12	0.07	1.53
177594	V0549 Lyr	42059528	7.85	7.85	6.28	285.15	1.44	0.04	0.03	0.77
178905		271523213	8.29	8.28	11.25	359.57	29.65	0.09	0.06	0.97
182634		122683109	15.04	13.42	3.69	249.51	1.07	0.05	0.03	0.90
184522	V2084 Cyg	138160886	11.36	11.37	10.16	122.89	0.22	0.09	0.05	1.81
185139	QQ Tel	143463658	15.31	15.54	8.37	102.07	0.31	0.06	0.04	1.15
185332	V1745 Cyg	213679825	18.73	25.58	1.06	140.54	0.43	0.04	0.03	1.66
186357	V1276 Cyg	216982075	11.36	12.11	1.18	84.32	0.09	0.17	0.06	1.74
186786	NZ Pav	339600902	12.50	13.71	4.54	59.45	0.15	0.08	0.04	2.08
187764	CN Dra	258388363	10.00	5.05	7.02	173.06	5.93	0.12	0.09	0.02
188136	CC Oct	346793769	8.01	8.01	10.08	193.48	3.58	0.14	0.09	1.40
188520	CE Oct	313552150	18.35	14.09	0.91	141.86	0.48	0.02	0.02	2.23
191635	V2109 Cyg	294598376	5.37	5.37	51.61	212.02	0.68	0.09	0.07	0.78
191804	IN Dra	269697721	7.29	7.29	6.94	217.90	1.22	0.11	0.05	1.20
191850		129277739	13.51	13.53	21.96	350.32	5.22	0.12	0.08	1.86
192518	NU Vul	452310756	5.32	5.33	6.53	95.98	0.55	0.04	0.03	0.25
192640	V1644 Cyg	10988057	37.45	37.43	5.21	40.74	0.13	0.04	0.03	1.86
192871	V0383 Vul	304501606	5.43	7.39	9.29	199.86	0.67	0.12	0.06	0.54
193084		164328483	17.86	1.95	1.89	424.33	6.45	0.01	0.01	-0.55
193138	IO Dra	403114672		8.73	4.74	185.71	3.45	0.13	0.07	1.34
194492	V0382 Pav	404239187	7.08	7.08	54.92	385.84	1.89	0.07	0.07	0.90
195961	ρ Pav	351535191	8.76	10.31	6.29	62.32	0.37	0.17	0.10	0.72
196517	V0342 Pav	387241049	29.41	32.50	0.69	167.70	0.48	0.03	0.04	2.31
196638	BU Mic	291112607	7.22	7.22	9.34	180.92	0.63	0.12	0.06	0.80
197100	V2129 Cyg	343264872	6.46	6.46	24.61	351.17	3.40	0.08	0.06	0.50
198830	BQ Ind	354171926	12.20	12.20	75.58	362.89	2.34	0.06	0.05	2.00
199434	V0388 Pav	372344502	6.32	6.32	15.02	302.80	1.48	0.07	0.06	1.28
199757	ZZ Mic	126659093	14.88	14.89	118.56	331.26	1.85	0.04	0.04	1.81
199908	DQ Cep	336444537	12.69	12.68	11.36	183.71	0.48	0.11	0.06	0.82
200925	V1719 Cyg	290277380	3.74	3.74	89.89	387.29	2.32	0.10	0.08	-0.05
205847	CF Ind	139825582	5.92	5.93	8.21	209.65	0.97	0.09	0.04	1.01
206553	CG Oct	419666736	15.87	8.18	7.14	103.72	0.16	0.07	0.04	1.41

Table 1 — continued from previous page

HD	Name	TIC	f_{cat} d^{-1}	f_1 d^{-1}	a_1 ppt	dist pc	e_dist pc	A_v mag	e_A_v mag	M_v mag
208435	BZ Gru	197686479	6.77	8.27	13.42	125.55	0.47	0.11	0.06	0.57
208664	BE Ind	394015973	21.19	21.89	1.89	224.12	1.44	0.04	0.03	1.40
208999	BX Ind	265566844	5.63	5.63	29.05	216.69	0.77	0.10	0.07	1.11
213204	UV PsA	253917376	8.77	9.15	6.82	215.40	1.22	0.10	0.06	1.63
213655	UW PsA	209362175	15.38	15.70	3.80	168.40	2.22	0.11	0.05	1.26
214441	CC Gru	161172103	8.01	7.93	9.73	119.78	0.28	0.13	0.06	1.13
217236	WX PsA	89464315	8.01	8.01	4.72	95.33	0.63	0.08	0.07	0.52
219586	V0388 Cep	427651165	3.68	4.30	8.29	114.92	0.49	0.07	0.05	0.18
219891		173771603	10.08	10.08	1.08	137.53	0.59	0.02	0.01	0.80
220237	V0459 Cep	326201430	5.59	5.59	6.81	210.54	0.62	0.14	0.06	0.86
220392	DQ Gru	469933721	4.68	4.58	7.38	125.18	0.54	0.06	0.03	0.57
220978	BS Scl	303584611	8.48	17.63	1.38	127.19	0.34	0.08	0.04	1.31
221142	V0377 Cep	461545977	13.70	15.34	6.19	123.95	0.24	0.05	0.04	1.11
223338	BS Aqr	9632550	5.06	5.05	113.31	528.98	10.56	0.09	0.08	0.66
223480	BF Phe	144387364	16.03	16.02	3.62	107.13	0.22	0.05	0.03	2.22
223661	V0396 And	177363174	9.55	9.55	10.04	216.87	1.49	0.15	0.06	1.03
224852		355687188	8.19	8.19	69.05	584.00	6.92	0.10	0.07	1.02
227695	V1821 Cyg	90350726	9.24	8.82	5.03	607.06	7.91	0.12	0.07	0.95
230990	V0336 Sge	343216782	5.43	6.22	6.52	474.43	5.92	0.10	0.07	0.82
254061		166979292	17.21	17.22	85.35	349.58	2.67	0.05	0.05	2.36
261331	V0588 Mon	220249462	7.14	5.14	4.51	578.77	5.33	0.05	0.03	0.91
261446	V0589 Mon	220281554	6.27	6.49	8.00	620.57	5.24	0.14	0.08	0.90
290764	V1247 Ori	11199521	10.31	10.31	5.62	401.20	2.77	0.05	0.04	1.75
290799	V1790 Ori	11361473	23.53	22.53	4.61	420.68	3.75	0.05	0.03	2.50
292962		33149129	9.19	9.19	73.63	486.18	3.75	0.06	0.05	1.41
339660	V0381 Vul	245151597	17.86	10.43	2.19	814.38	28.26	0.06	0.06	0.56
—	AB Cas	354922610	17.15	17.16	12.50	329.74	1.47	0.11	0.10	2.59
—	AE UMa	357132618	11.63	11.63	135.36	735.57	16.08	0.09	0.07	1.93
—	AI Hya	455178154	7.25	6.24	4.48	611.24	6.20	0.12	0.07	0.31
—	AN Lyn	56882581	10.17	10.18	49.73	666.20	10.31	0.09	0.07	1.44
—	BO Lyn	99091734	10.71	10.71	59.53	1343.42	29.97	0.06	0.06	0.79
—	CC And	191466237	8.01	8.00	41.76	379.57	2.26	0.08	0.07	1.37
—	DE Lac	119486942	3.94	3.94	83.84	765.00	10.25	0.17	0.12	0.75
—	GP And	436546358	12.71	12.71	157.14	545.24	7.66	0.09	0.08	2.03
—	GW Dra	329153513	7.92	7.92	17.10	358.69	2.04	0.10	0.07	1.40
—	GW UMa	150276417	4.92	4.92	115.35	676.48	21.37	0.20	0.13	0.34
—	OS Gem	171300396	15.48	14.50	1.02	453.16	2.79	0.04	0.03	1.06
—	RS Gru	139845816	6.80	6.80	146.38	245.74	1.18	0.05	0.05	1.26
—	UV Tri	61275530	10.00	9.33	13.37	710.73	15.91	0.08	0.06	1.81
—	UY Cam	441619744	3.75	3.75	106.88	1425.46	31.72	0.07	0.06	0.69
—	V0361 And	186297798	8.76	8.77	7.16	238.84	1.45	0.11	0.07	0.74
—	V0402 Cep	468294062	8.14	8.13	6.67	630.06	4.41	0.15	0.09	1.40
—	V0420 Car	364398340		16.03	0.74	423.76	8.31	0.07	0.04	2.18
—	V0421 Car	364398097		39.12	1.95	411.41	1.82	0.05	0.03	2.75
—	V0459 Per	259254245	27.03	22.48	1.63	174.82	0.44	0.11	0.05	2.86
—	V0593 Lyr	289325437	9.79	9.79	177.11	1459.59	25.88	0.09	0.07	0.77
—	V0798 Cyg	69546708	5.13	5.14	136.89	2450.28	51.23	0.09	0.07	0.96
—	V0830 Her	308407544	5.56	5.65	32.49	466.45	2.58	0.12	0.09	0.82
—	V1162 Ori	34512862	12.71	12.71	39.27	444.01	4.65	0.08	0.07	1.67
—	V1199 Ori	43846109		13.03	2.87	608.61	6.48	0.10	0.05	2.69
—	VX Hya	289711518	4.48	4.48	89.84	932.72	12.68	0.07	0.07	0.68
—	XX Cyg	233310793	7.41	7.41	226.32	1162.39	20.23	0.11	0.09	1.43
—	XX Pyx	37366830	38.17	38.11	6.71	703.30	13.90	0.06	0.04	2.21
—	YZ Boo	233465540	9.61	9.61	113.12	585.02	4.71	0.06	0.05	1.62
—		293110952	14.20	14.20	33.48	421.82	8.48	0.06	0.05	2.71
—		308456254	6.28	6.28	41.62	706.94	11.11	0.11	0.09	1.57
—		262652067	5.63	5.63	63.28	726.83	5.89	0.15	0.11	1.37
—		362384415	7.22	7.22	140.85	1161.49	30.53	0.11	0.09	1.68
—		278003738	8.55	8.55	23.55	560.78	4.72	0.09	0.07	1.89

Table 1 — continued from previous page

HD	Name	TIC	f_{cat} d^{-1}	f_1 d^{-1}	a_1 ppt	dist pc	e_dist pc	A_v mag	e_A_v mag	M_v mag
—		260842067	5.36	5.36	52.04	548.38	4.30	0.05	0.04	1.28
—		90185615	7.20	7.20	63.17	578.33	5.45	0.13	0.12	1.63
—		298112357	9.84	9.85	191.32	595.38	5.16	0.12	0.10	1.96
—		60405689	14.99	14.99	57.89	567.84	5.83	0.08	0.06	2.48
—		339675323	7.45	7.45	64.11	936.41	18.04	0.16	0.12	1.58
—		130474019	12.29	12.28	116.85	975.66	10.18	0.08	0.07	2.20
—		431589510	7.73	7.73	82.23	1356.52	138.29	0.10	0.09	1.60
—		264482621	18.80	18.78	36.88	392.61	2.46	0.08	0.09	2.71
—		200624064	5.23	5.23	117.86	1088.42	73.67	0.28	0.17	1.04
—		46937596	7.89	7.89	76.77	811.80	10.99	0.09	0.08	1.54
—		168384036	9.25	9.26	111.20	576.54	7.62	0.09	0.08	1.73
—		135362719	8.65	8.65	13.38	230.41	0.81	0.08	0.06	1.56
—		65138566	18.35	18.33	33.18	538.03	5.08	0.06	0.05	2.48
—		308396022	13.21	13.20	72.74	600.99	10.85	0.10	0.09	2.01
—		181087723	7.72	7.72	112.18	1450.15	25.54	0.11	0.09	1.33
—		391474560	10.54	10.54	94.50	1122.74	11.83	0.10	0.08	1.70
—		9524429	31.06	15.02	1.59	62.09	0.43	0.04	0.03	2.14
—		142945544	16.47	18.48	70.25	463.26	9.86	0.05	0.05	2.40
—		410038602	13.07	13.07	57.78	1163.57	23.90	0.06	0.05	1.92
—		178616716	9.77	9.76	94.65	1224.71	23.01	0.11	0.10	1.43
—		155128092	14.68	14.68	122.04	775.74	12.54	0.06	0.05	1.90
—		100701385	4.61	5.50	4.07	119.66	0.36	0.14	0.07	0.64
—		90322352	9.33	9.33	114.45	1074.32	29.73	0.08	0.08	1.29
—		148357344	11.10	11.10	183.35	1229.90	21.70	0.15	0.11	1.51
—		78850814	9.12	9.12	71.27	1099.34	10.85	0.15	0.11	1.25
—		393420032	6.01	6.01	62.76	1204.71	25.86	0.15	0.10	0.69
—		360736543	6.71	6.71	52.99	1393.52	29.54	0.08	0.07	0.82
—		261089835	7.15	11.16	82.29	1226.34	28.75	0.14	0.11	1.32
—		396855479	9.09	9.47	2.68	486.62	3.05	0.12	0.05	1.06
—		100708841		30.46	1.38	24.20	0.06	0.04	0.04	2.54
—		323292655	12.50	11.62	1.97	98.63	0.18	0.06	0.06	1.06
—		468184895	10.31	10.49	10.04	90.07	0.45	0.08	0.05	0.59
—		589826	47.62	48.09	1.16	57.13	0.06	0.04	0.03	2.35
—		333375443	22.73	22.26	1.90	76.63	0.25	0.07	0.04	1.08
—		357040880	33.33	33.28	4.40	106.52	0.43	0.03	0.03	1.43
—		13972612	9.60	10.61	4.49	1778.09	26.62	0.22	0.10	-0.49
—		301407485	58.82	59.03	1.42	210.64	1.44	0.03	0.03	1.66
—		13332837	6.87	6.88	9.24	1670.61	26.69	0.11	0.07	-1.42

This paper has been typeset from a TEX/LATEX file prepared by the author.